Auger and radiative decay rates of $1s$ vacancy states in the boron isoelectronic sequence: Effects of relativity and configuration interaction

Mau Hsiung Chen

University of California, Lawrence Livermore National Laboratory, Livermore, California 94550

Bernd Crasemann

Department of Physics and Chemical Physics Institute, University of Oregon, Eugene, Oregon 97403
(Received 15 December 1986)

Wavelengths, radiative transition probabilities, Auger energies, and Auger rates have been calculated relativistically for $1s2s^22p^2$, $1s2s2p^3$, and $1s2p^4$ configurations of the boron isoelectronic sequence, in terms of the multiconfiguration Dirac-Fock model. Ions with atomic numbers from $Z=6$ to 54 are included. The generalized Breit interaction, quantum-electrodynamic corrections, and relaxation are taken into account in the calculations of transition energies. Transition rates are computed in intermediate coupling, including configuration interaction within the same complex. It is found that the effects of relativity play a major role in the forbidden transitions, and also become quite important for allowed transitions for $Z \geq 20$. Configuration interaction is found to affect transition rates by as much as a factor of 2 for light ions.

I. INTRODUCTION

The properties of multiply ionized atoms are very important in connection with astrophysical problems and with the physics of atomic collisions, fusion plasmas, and x-ray lasers. Knowledge of the decay rates of autoionizing states of highly ionized atoms is essential for the determination of dielectronic satellite spectra and of total dielectronic recombination coefficients. The Auger and x-ray transitions of the He, Li, and Be isoelectronic sequences have recently been investigated.[1-5] In this paper, we report on relativistic calculations of Auger and x-ray transition rates for each multiplet state of B-like ions. The calculations were performed in intermediate coupling with configuration interaction, using the multiconfiguration Dirac-Fock (MCDF) model,[5,6] for the $1s2s^22p^2$, $1s2s2p^3$, and $1s2p^4$ configurations of 15 elements with atomic numbers $6 \leq Z \leq 54$. The effects of relativity and configuration interaction on the radiative and radiationless transition rates were studied by comparing the results from relativistic, nonrelativistic, multiconfiguration, and single-configuration calculations.

II. THEORETICAL METHOD

A. Relativistic Auger rates

Auger transition probabilities were calculated from perturbation theory.[7,8] The transition rate in the frozen-orbital approximation is

$$T = \frac{2\pi}{\hbar} \left| \left\langle \psi_f \left| \sum_{\substack{\alpha,\beta \\ (\alpha < \beta)}} V_{\alpha\beta} \right| \psi_i \right\rangle \right|^2 \rho(\varepsilon) \ . \tag{1}$$

Here, ψ_i and ψ_f are the antisymmetrized many-electron wave functions of the initial and final states of the ion, respectively; $\rho(\varepsilon)$ is the energy density of final states.

In the present work, the two-electron operator $V_{\alpha\beta}$ in Eq. (1) is taken to be the sum of the Coulomb and generalized Breit operators:[9]

$$V_{12} = \frac{1}{r_{12}} - \boldsymbol{\alpha}_1 \cdot \boldsymbol{\alpha}_2 \frac{\cos(\omega r_{12})}{r_{12}}$$
$$+ (\boldsymbol{\alpha}_1 \cdot \boldsymbol{\nabla}_1)(\boldsymbol{\alpha}_2 \cdot \boldsymbol{\nabla}_2) \frac{\cos(\omega r_{12}) - 1}{\omega^2 r_{12}} \ , \tag{2}$$

where the $\boldsymbol{\alpha}_i$ are Dirac matrices and ω is the wave number of the exchange virtual photon. In Eq. (2) and hereafter, atomic units are used unless specified otherwise.

In the MCDF model,[6] an atomic state function (ASF) for a state i with total angular momentum JM is expanded in terms of the configuration state functions (CSF's):

$$\psi_i(JM) = \sum_{\lambda=1}^n C_{i\lambda} \Phi(\Gamma_\lambda JM) \ , \tag{3}$$

where n is the number of CFS's included in the expansion, and the $C_{i\lambda}$ are the mixing coefficients for the state i.

The Auger transition rate from an initial ionic state i to the final ionic state f is then given by[5]

$$A_a(i \rightarrow f) = \sum_{\kappa_c} \left| \sum_\lambda \sum_{\lambda'} C_{i\lambda} C_{f\lambda'} \left\langle \Phi(\Gamma_{\lambda'} J'M') \varepsilon \kappa_c ; JM \left| \sum_{\substack{\alpha,\beta \\ (\alpha<\beta)}} V_{\alpha\beta} \right| \Phi(\Gamma_\lambda JM) \right\rangle \right|^2 \ . \tag{4}$$

Here, the continuum wave function $\varepsilon \kappa_c$ is normalized to represent one ejected electron per unit time, and we have $\kappa_c = (l_c - j_c)(2j_c + 1)$.

TABLE I. Total Auger and radiative rates (in sec⁻¹) for states of the $1s2s^22p^2$ configuration of boronlike ions. Numbers in square brackets indicate power of ten.

Ion	$^4P_{1/2}$ Auger	$^4P_{1/2}$ X-ray	$^4P_{3/2}$ Auger	$^4P_{3/2}$ X-ray	$^4P_{5/2}$ Auger	$^4P_{5/2}$ X-ray	$^2D_{3/2}$ Auger	$^2D_{3/2}$ X-ray	$^2D_{5/2}$ Auger	$^2D_{5/2}$ X-ray	$^2P_{1/2}$ Auger	$^2P_{1/2}$ X-ray	$^2P_{3/2}$ Auger	$^2P_{3/2}$ X-ray	$^2S_{1/2}$ Auger	$^2S_{1/2}$ X-ray
$_6$C^{1+}	1.02[14]	1.82[7]	1.02[14]	5.08[9]	1.01[14]	5.15[9]	1.25[14]	2.68[11]	1.35[14]	2.09[11]	6.59[13]	6.18[11]	7.54[13]	5.59[11]	1.26[14]	2.27[11]
$_7$N^{2+}	1.23[14]	5.55[7]	1.23[14]	1.13[10]	1.22[14]	1.14[10]	1.66[14]	4.97[11]	1.66[14]	4.92[11]	7.64[13]	1.46[12]	7.67[13]	1.45[12]	1.52[14]	5.32[11]
$_8$O^{3+}	1.40[14]	1.75[8]	1.40[14]	2.20[10]	1.40[14]	2.23[10]	1.92[14]	1.00[12]	1.93[14]	9.94[11]	8.54[13]	2.95[12]	8.55[13]	2.94[12]	1.75[14]	1.07[12]
$_9$F^{4+}	1.55[14]	5.33[8]	1.54[14]	3.89[10]	1.54[14]	3.94[10]	2.14[14]	1.82[12]	2.15[14]	1.80[12]	9.26[13]	5.36[12]	9.28[13]	5.34[12]	1.93[14]	1.94[12]
$_{10}$Ne^{5+}	1.67[14]	1.53[9]	1.66[14]	6.40[10]	1.66[14]	6.51[10]	2.33[14]	3.07[12]	2.34[14]	3.03[12]	9.94[13]	8.98[12]	9.96[13]	8.96[12]	2.08[14]	3.25[12]
$_{12}$Mg^{7+}	1.86[14]	1.02[10]	1.85[14]	1.50[11]	1.86[14]	1.54[11]	2.61[14]	7.43[12]	2.64[14]	7.20[12]	1.11[14]	2.13[13]	1.11[14]	2.12[13]	2.32[14]	7.79[12]
$_{14}$Si^{9+}	2.01[14]	5.17[10]	2.00[14]	3.08[11]	2.01[14]	3.29[11]	2.81[14]	1.56[13]	2.87[14]	1.46[13]	1.21[14]	4.30[13]	1.23[14]	4.27[13]	2.49[14]	1.61[13]
$_{16}$S^{11+}	2.14[14]	2.12[11]	2.12[14]	5.92[11]	2.13[14]	6.75[11]	2.94[14]	2.98[13]	3.05[14]	2.66[13]	1.32[14]	7.76[13]	1.34[14]	7.65[13]	2.60[14]	3.03[13]
$_{18}$Ar^{13+}	2.25[14]	7.36[11]	2.23[14]	1.11[12]	2.25[14]	1.41[12]	3.02[14]	5.34[13]	3.20[14]	4.47[13]	1.42[14]	1.29[14]	1.47[14]	1.26[14]	2.68[14]	5.28[13]
$_{20}$Ca^{15+}	2.34[14]	2.22[12]	2.31[14]	2.04[12]	2.35[14]	3.08[12]	3.07[14]	9.03[13]	3.32[14]	7.00[13]	1.51[14]	2.00[14]	1.59[14]	1.94[14]	2.73[14]	8.62[13]
$_{22}$Ti^{17+}	2.46[14]	5.94[12]	2.41[14]	3.75[12]	2.48[14]	6.85[12]	3.12[14]	1.45[14]	3.45[14]	1.04[14]	1.61[14]	2.97[14]	1.73[14]	2.83[14]	2.80[14]	1.33[14]
$_{26}$Fe^{21+}	2.63[14]	3.40[13]	2.55[14]	1.19[13]	2.73[14]	3.12[13]	3.15[14]	3.27[14]	3.55[14]	1.95[14]	1.76[14]	5.85[14]	1.97[14]	5.44[14]	2.87[14]	2.76[14]
$_{30}$Zn^{25+}	2.79[14]	1.18[14]	2.68[14]	3.30[13]	3.03[14]	1.06[14]	3.21[14]	6.35[14]	3.58[14]	3.09[14]	1.90[14]	1.02[15]	2.16[14]	9.46[14]	2.96[14]	4.97[14]
$_{36}$Kr^{31+}	3.12[14]	4.59[14]	2.93[14]	1.15[14]	3.55[14]	3.74[14]	3.40[14]	1.42[15]	3.67[14]	5.15[14]	2.19[14]	2.02[15]	2.44[14]	1.92[15]	3.18[14]	1.02[15]
$_{42}$Mo^{37+}	3.45[14]	1.17[15]	3.18[14]	3.11[14]	4.01[14]	8.80[14]	3.64[14]	2.73[15]	3.82[14]	8.07[14]	2.49[14]	3.60[15]	2.66[14]	3.49[15]	3.38[14]	1.84[15]
$_{47}$Ag^{42+}	3.80[14]	2.13[15]	3.42[14]	6.23[14]	4.39[14]	1.53[15]	3.88[14]	4.31[15]	4.00[14]	1.15[15]	2.78[14]	5.54[15]	2.83[14]	5.41[15]	3.55[14]	2.83[15]
$_{54}$Xe^{49+}	4.46[14]	4.19[15]	3.88[14]	1.45[15]	5.02[14]	2.90[15]	4.33[14]	7.43[15]	4.35[14]	1.84[15]	3.33[14]	9.49[15]	3.13[14]	9.30[15]	3.88[14]	4.82[15]

TABLE II. Total Auger and radiative rates (in sec⁻¹) for states of the $1s2s2p^3$ configuration of boronlike ions. Numbers in square brackets indicate power of ten.

Ion	$(^3S)^6S_{5/2}$ Auger	$(^3S)^6S_{5/2}$ X-ray	$(^3S)^4D_{1/2}$ Auger	$(^3S)^4D_{1/2}$ X-ray	$(^3S)^4D_{3/2}$ Auger	$(^3S)^4D_{3/2}$ X-ray	$(^3S)^4D_{5/2}$ Auger	$(^3S)^4D_{5/2}$ X-ray	$(^3S)^4D_{7/2}$ Auger	$(^3S)^4D_{7/2}$ X-ray	$(^3S)^4S_{3/2}$ Auger	$(^3S)^4S_{3/2}$ X-ray	$(^3S)^2S_{1/2}$ Auger	$(^3S)^2S_{1/2}$ X-ray
$_6$C^{1+}	1.93[9]	6.42[6]	7.23[13]	2.04[11]	7.23[13]	2.05[11]	7.23[13]	2.05[11]	7.26[13]	2.07[11]	3.78[13]	7.90[11]	1.35[13]	8.35[11]
$_7$N^{2+}	2.15[9]	1.49[7]	9.49[13]	4.80[11]	9.50[13]	4.81[11]	9.53[13]	4.83[11]	9.58[13]	4.85[11]	3.89[13]	1.87[12]	3.49[13]	1.81[12]
$_8$O^{3+}	3.02[9]	3.91[7]	1.15[14]	9.69[11]	1.15[14]	9.71[11]	1.15[14]	9.73[11]	1.16[14]	9.77[11]	3.92[13]	3.78[12]	5.06[13]	3.49[12]
$_9$F^{4+}	4.81[9]	1.08[8]	1.32[14]	1.76[12]	1.32[14]	1.76[12]	1.32[14]	1.77[12]	1.32[14]	1.77[12]	3.92[13]	6.87[12]	4.69[13]	6.70[12]
$_{10}$Ne^{5+}	8.19[9]	2.93[8]	1.46[14]	2.95[12]	1.46[14]	2.96[12]	1.46[14]	2.96[12]	1.47[14]	2.97[12]	3.92[13]	1.16[13]	5.29[13]	1.12[13]
$_{12}$Mg^{7+}	2.40[10]	1.87[9]	1.69[14]	7.03[12]	1.68[14]	7.09[12]	1.69[14]	7.05[12]	1.69[14]	7.07[12]	3.94[13]	2.75[13]	7.05[13]	2.59[13]
$_{14}$Si^{9+}	6.60[10]	9.52[9]	1.85[14]	1.43[13]	1.84[14]	1.45[13]	1.85[14]	1.44[13]	1.86[14]	1.44[13]	4.03[13]	5.60[13]	9.17[13]	5.02[13]
$_{16}$S^{11+}	1.63[11]	3.96[10]	1.98[14]	2.62[13]	1.96[14]	2.67[13]	1.97[14]	2.62[13]	2.00[14]	2.63[13]	4.18[13]	1.02[14]	1.13[14]	8.66[13]
$_{18}$Ar^{13+}	3.69[11]	1.40[11]	2.08[14]	4.44[13]	2.04[14]	4.64[13]	2.07[14]	4.43[13]	2.10[14]	4.44[13]	4.63[13]	1.70[14]	1.31[14]	1.39[14]
$_{20}$Ca^{15+}	7.69[11]	4.33[11]	2.16[14]	7.09[13]	2.07[14]	7.85[13]	2.14[14]	7.04[13]	2.19[14]	7.05[13]	5.44[13]	2.62[14]	1.44[14]	2.13[14]
$_{22}$Ti^{17+}	1.49[12]	1.20[12]	2.22[14]	1.08[14]	2.05[14]	1.31[14]	2.19[14]	1.07[14]	2.27[14]	1.07[14]	7.31[13]	3.79[14]	1.51[14]	3.14[14]
$_{26}$Fe^{21+}	4.78[12]	7.20[12]	2.29[14]	2.31[14]	1.92[14]	3.32[14]	2.22[14]	2.20[14]	2.38[14]	2.19[14]	1.07[14]	6.69[14]	1.58[14]	6.29[14]
$_{30}$Zn^{25+}	1.29[13]	3.33[13]	2.32[14]	4.60[14]	1.84[14]	6.91[14]	2.20[14]	4.03[14]	2.46[14]	4.02[14]	1.48[14]	1.17[15]	1.57[14]	1.14[15]
$_{36}$Kr^{31+}	4.09[13]	2.13[14]	2.28[14]	1.19[15]	1.83[14]	1.63[15]	2.01[14]	8.14[14]	2.53[14]	8.66[14]	3.06[14]	2.02[15]	1.53[14]	2.41[15]
$_{42}$Mo^{37+}	8.07[13]	7.87[14]	2.22[14]	2.72[15]	1.89[14]	3.22[15]	1.71[14]	1.35[15]	2.59[14]	1.65[15]	4.81[14]	2.87[15]	1.51[14]	4.40[15]
$_{47}$Ag^{42+}	1.07[14]	1.68[15]	2.18[14]	4.83[15]	1.94[14]	5.23[15]	1.53[14]	1.95[15]	2.63[14]	2.63[15]	5.73[14]	4.06[15]	1.49[14]	6.76[15]
$_{54}$Xe^{49+}	1.30[14]	3.66[15]	2.15[14]	9.37[15]	2.03[14]	9.34[15]	1.41[14]	3.23[15]	2.68[14]	4.65[15]	6.93[14]	6.71[15]	1.45[14]	1.14[16]

TABLE II. (Continued).

Ion	$(^3S)^4P_{1/2}$ Auger	X-ray	$(^3S)^4P_{3/2}$ Auger	X-ray	$(^3S)^4P_{5/2}$ Auger	X-ray	$(^3S)^2D_{3/2}$ Auger	X-ray	$(^3S)^2D_{5/2}$ Auger	X-ray	$(^3S)^2P_{1/2}$ Auger	X-ray	$(^3S)^2P_{3/2}$ Auger	X-ray
$_6C^{1+}$	5.66[13]	2.10[11]	5.67[13]	2.10[11]	5.67[13]	2.11[11]	1.25[14]	5.71[11]	1.25[14]	5.70[11]	1.09[14]	5.77[11]	1.08[14]	5.77[11]
$_7N^{2+}$	7.37[13]	4.92[11]	7.39[13]	4.93[11]	7.40[13]	4.94[11]	1.53[14]	1.34[12]	1.53[14]	1.34[12]	1.31[14]	1.36[12]	1.31[14]	1.36[12]
$_8O^{3+}$	8.88[13]	9.90[11]	8.90[13]	9.92[11]	8.91[13]	9.94[11]	1.76[14]	2.72[12]	1.76[14]	2.71[12]	1.50[14]	2.74[12]	1.50[14]	2.74[12]
$_9F^{4+}$	1.02[14]	1.79[12]	1.02[14]	1.80[12]	1.01[14]	1.80[12]	1.96[14]	4.93[12]	1.95[14]	4.93[12]	1.66[14]	4.97[12]	1.65[14]	4.97[12]
$_{10}Ne^{5+}$	1.12[14]	3.00[12]	1.12[14]	3.01[12]	1.12[14]	3.01[12]	2.12[14]	8.29[12]	2.12[14]	8.29[12]	1.79[14]	8.34[12]	1.78[14]	8.34[12]
$_{12}Mg^{7+}$	1.29[14]	7.13[12]	1.30[14]	7.15[12]	1.30[14]	7.16[12]	2.39[14]	1.98[13]	2.38[14]	1.98[13]	1.99[14]	1.99[13]	1.98[14]	1.79[13]
$_{14}Si^{9+}$	1.42[14]	1.45[13]	1.42[14]	1.46[13]	1.42[14]	1.46[13]	2.59[14]	4.03[13]	2.57[14]	4.04[13]	2.14[14]	4.06[13]	2.13[14]	3.93[13]
$_{16}S^{11+}$	1.51[14]	2.64[13]	1.52[14]	2.70[13]	1.53[14]	2.67[13]	2.75[14]	7.36[13]	2.71[14]	7.39[13]	2.25[14]	7.45[13]	2.28[14]	7.10[13]
$_{18}Ar^{13+}$	1.59[14]	4.46[13]	1.60[14]	4.64[13]	1.61[14]	4.54[13]	2.90[14]	1.24[14]	2.84[14]	1.25[14]	2.34[14]	1.26[14]	2.43[14]	1.15[14]
$_{20}Ca^{15+}$	1.66[14]	7.08[13]	1.66[14]	7.61[13]	1.69[14]	7.30[13]	3.05[14]	1.94[14]	2.94[14]	1.97[14]	2.39[14]	2.02[14]	2.57[14]	1.74[14]
$_{22}Ti^{17+}$	1.70[14]	1.07[14]	1.73[14]	1.20[14]	1.76[14]	1.13[14]	3.30[14]	2.86[14]	3.11[14]	2.95[14]	2.46[14]	3.09[14]	2.74[14]	2.47[14]
$_{26}Fe^{21+}$	1.78[14]	2.21[14]	1.92[14]	2.59[14]	1.89[14]	2.52[14]	3.60[14]	5.23[14]	3.31[14]	5.74[14]	2.33[14]	6.55[14]	2.86[14]	4.59[14]
$_{30}Zn^{25+}$	1.84[14]	4.14[14]	2.40[14]	4.91[14]	2.04[14]	5.39[14]	3.49[14]	8.02[14]	3.67[14]	9.30[14]	2.06[14]	1.24[15]	2.95[14]	7.92[14]
$_{36}Kr^{31+}$	1.90[14]	9.37[14]	2.70[14]	1.39[15]	2.24[14]	1.48[15]	2.60[14]	1.42[15]	4.82[14]	1.43[15]	1.72[14]	2.64[15]	3.12[14]	1.58[15]
$_{42}Mo^{37+}$	1.93[14]	1.87[15]	1.98[14]	3.42[15]	2.38[14]	3.19[15]	2.30[14]	2.62[15]	5.71[14]	2.21[15]	1.57[14]	4.76[15]	3.40[14]	2.63[15]
$_{47}Ag^{42+}$	1.94[14]	3.08[15]	1.80[14]	5.80[15]	2.40[14]	5.25[15]	2.19[14]	4.22[15]	6.21[14]	3.36[15]	1.52[14]	7.29[15]	3.74[14]	3.62[15]
$_{54}Xe^{49+}$	2.00[14]	5.59[15]	1.79[14]	1.05[16]	2.43[14]	9.30[15]	2.15[14]	7.56[15]	6.90[14]	5.89[15]	1.49[14]	1.24[16]	4.29[14]	5.35[15]

Ion	$(^1S)^4S_{3/2}$ Auger	X-ray	$(^1S)^2D_{3/2}$ Auger	X-ray	$(^1S)^2D_{5/2}$ Auger	X-ray	$(^1S)^2P_{1/2}$ Auger	X-ray	$(^1S)^2P_{3/2}$ Auger	X-ray
$_6C^{1+}$	8.91[13]	2.85[10]	1.38[14]	2.49[11]	1.38[14]	2.51[11]	1.21[14]	2.60[11]	1.22[14]	2.59[11]
$_7N^{2+}$	1.10[14]	5.83[10]	1.73[14]	5.82[11]	1.74[14]	5.86[11]	1.52[14]	5.99[11]	1.37[14]	7.47[11]
$_8O^{3+}$	1.28[14]	1.08[11]	2.04[14]	1.17[12]	2.04[14]	1.17[12]	1.54[14]	1.64[12]	1.78[14]	1.20[12]
$_9F^{4+}$	1.43[14]	1.86[11]	2.30[14]	2.11[12]	2.30[14]	2.12[12]	1.85[14]	2.59[12]	2.00[14]	2.15[12]
$_{10}Ne^{5+}$	1.56[14]	3.06[11]	2.52[14]	3.54[12]	2.53[14]	3.55[12]	2.03[14]	4.31[12]	2.18[14]	3.59[12]
$_{12}Mg^{7+}$	1.76[14]	2.68[12]	2.86[14]	8.45[12]	2.88[14]	8.39[12]	2.24[14]	1.10[13]	2.48[14]	8.46[12]
$_{14}Si^{9+}$	1.94[14]	2.28[12]	3.10[14]	1.75[13]	3.15[14]	1.70[13]	2.32[14]	2.48[13]	2.72[14]	1.70[13]
$_{16}S^{11+}$	2.06[14]	3.68[12]	3.24[14]	3.38[13]	3.37[14]	3.09[13]	2.34[14]	4.98[13]	2.91[14]	3.06[13]
$_{18}Ar^{13+}$	2.19[14]	7.01[12]	3.30[14]	6.23[13]	3.55[14]	5.18[13]	2.37[14]	9.01[13]	3.08[14]	5.04[13]
$_{20}Ca^{15+}$	2.29[14]	1.43[13]	3.27[14]	1.10[14]	3.69[14]	8.19[13]	2.42[14]	1.49[14]	3.23[14]	7.64[13]
$_{22}Ti^{17+}$	2.44[14]	3.08[13]	3.24[14]	1.84[14]	3.88[14]	1.24[14]	2.57[14]	2.27[14]	3.46[14]	1.12[14]
$_{26}Fe^{21+}$	2.58[14]	1.36[14]	2.96[14]	4.37[14]	4.00[14]	2.57[14]	2.96[14]	4.46[14]	3.78[14]	2.10[14]
$_{30}Zn^{25+}$	2.67[14]	4.26[14]	2.65[14]	8.54[14]	3.86[14]	4.97[14]	3.53[14]	7.42[14]	4.04[14]	3.73[14]
$_{36}Kr^{31+}$	2.92[14]	1.27[15]	2.25[14]	1.87[15]	2.98[14]	1.22[15]	4.40[14]	1.40[15]	4.37[14]	8.37[14]
$_{42}Mo^{37+}$	3.18[14]	2.80[15]	1.96[14]	3.50[15]	2.37[14]	2.25[15]	5.01[14]	2.48[15]	4.58[14]	1.69[15]
$_{47}Ag^{42+}$	3.28[14]	4.96[15]	1.78[14]	5.47[15]	2.16[14]	3.33[15]	5.45[14]	3.82[15]	4.74[14]	2.80[15]
$_{54}Xe^{49+}$	3.34[14]	9.67[15]	1.61[14]	9.41[15]	2.03[14]	5.40[15]	6.08[14]	6.55[15]	4.98[14]	5.16[15]

TABLE III. Total Auger and radiative rates (in sec⁻¹) for states of the $1s2p^4$ configuration of boronlike ions. Numbers in square brackets indicate power of ten.

Ion	$^4P_{1/2}$ Auger	$^4P_{1/2}$ X-ray	$^4P_{3/2}$ Auger	$^4P_{3/2}$ X-ray	$^4P_{5/2}$ Auger	$^4P_{5/2}$ X-ray	$^2D_{3/2}$ Auger	$^2D_{3/2}$ X-ray	$^2D_{5/2}$ Auger	$^2D_{5/2}$ X-ray	$^2P_{1/2}$ Auger	$^2P_{1/2}$ X-ray	$^2P_{3/2}$ Auger	$^2P_{3/2}$ X-ray	$^2S_{1/2}$ Auger	$^2S_{1/2}$ X-ray
$_6$C^{1+}	7.82[13]	2.05[11]	7.84[13]	2.06[11]	7.90[13]	2.03[11]	1.24[14]	4.09[11]	1.24[14]	4.11[11]	7.61[13]	8.24[11]	7.66[13]	8.24[11]	8.45[13]	4.12[11]
$_7$N^{2+}	1.02[14]	4.75[11]	1.03[14]	4.77[11]	1.04[14]	4.73[11]	1.62[14]	9.57[11]	1.63[14]	9.60[11]	1.00[14]	1.93[12]	1.00[14]	1.93[12]	1.11[14]	9.56[11]
$_8$O^{3+}	1.23[14]	9.54[11]	1.24[14]	9.57[11]	1.25[14]	9.55[11]	1.95[14]	1.93[12]	1.96[14]	1.93[12]	1.21[14]	3.88[12]	1.21[14]	3.88[12]	1.34[14]	1.92[12]
$_9$F^{4+}	1.41[14]	1.73[12]	1.41[14]	1.73[12]	1.41[14]	1.73[12]	2.22[14]	3.50[12]	2.22[14]	3.50[12]	1.37[14]	7.03[12]	1.38[14]	7.02[12]	1.53[14]	3.46[12]
$_{10}$Ne^{5+}	1.56[14]	2.89[12]	1.56[14]	2.90[12]	1.57[14]	2.90[12]	2.46[14]	5.88[12]	2.46[14]	5.86[12]	1.52[14]	1.18[13]	1.53[14]	1.18[13]	1.69[14]	5.79[12]
$_{12}$Mg^{7+}	1.80[14]	6.88[12]	1.80[14]	6.89[12]	1.81[14]	6.91[12]	2.82[14]	1.41[13]	2.84[14]	1.39[13]	1.76[14]	2.80[13]	1.78[14]	2.78[13]	1.96[14]	1.38[13]
$_{14}$Si^{9+}	1.97[14]	1.40[13]	1.97[14]	1.40[13]	1.99[14]	1.41[13]	3.07[14]	2.94[13]	3.12[14]	2.84[13]	1.94[14]	5.71[13]	1.98[14]	5.60[13]	2.15[14]	2.80[13]
$_{16}$S^{11+}	2.11[14]	2.57[13]	2.10[14]	2.57[13]	2.14[14]	2.58[13]	3.23[14]	5.59[13]	3.34[14]	5.18[13]	2.08[14]	1.04[14]	2.17[14]	1.00[14]	2.31[14]	5.13[13]
$_{18}$Ar^{13+}	2.21[14]	4.35[13]	2.21[14]	4.36[13]	2.25[14]	4.38[13]	3.31[14]	1.00[14]	3.51[14]	8.73[13]	2.20[14]	1.75[14]	2.37[14]	1.63[14]	2.43[14]	8.72[13]
$_{20}$Ca^{15+}	2.31[14]	6.95[13]	2.30[14]	7.00[13]	2.35[14]	7.00[13]	3.33[14]	1.70[14]	3.65[14]	1.38[14]	2.30[14]	2.75[14]	2.57[14]	2.47[14]	2.52[14]	1.40[14]
$_{22}$Ti^{17+}	2.40[14]	1.06[14]	2.39[14]	1.08[14]	2.46[14]	1.07[14]	3.34[14]	2.72[14]	3.79[14]	2.08[14]	2.41[14]	4.11[14]	2.79[14]	3.56[14]	2.61[14]	2.17[14]
$_{26}$Fe^{21+}	2.53[14]	2.28[14]	2.54[14]	2.51[14]	2.62[14]	2.27[14]	3.26[14]	5.87[14]	3.93[14]	4.20[14]	2.56[14]	8.03[14]	3.09[14]	6.73[14]	2.69[14]	4.75[14]
$_{30}$Zn^{25+}	2.65[14]	4.66[14]	2.76[14]	6.29[14]	2.78[14]	4.34[14]	3.10[14]	9.72[14]	4.02[14]	7.56[14]	2.68[14]	1.39[15]	3.29[14]	1.17[15]	2.74[14]	9.14[14]
$_{36}$Kr^{31+}	2.84[14]	1.28[15]	3.08[14]	2.03[15]	2.96[14]	9.95[14]	2.87[14]	1.52[15]	4.08[14]	1.57[15]	2.76[14]	2.70[15]	3.45[14]	2.40[15]	2.78[14]	1.97[15]
$_{42}$Mo^{37+}	3.01[14]	2.84[15]	3.23[14]	4.39[15]	3.12[14]	1.98[15]	2.80[14]	2.47[15]	4.14[14]	2.90[15]	2.82[14]	4.86[15]	3.53[14]	4.43[15]	2.81[14]	3.60[15]
$_{47}$Ag^{42+}	3.10[14]	4.78[15]	3.31[14]	7.28[15]	3.21[14]	3.25[15]	2.78[14]	3.75[15]	4.19[14]	4.53[15]	2.86[14]	7.62[15]	3.54[14]	6.91[15]	2.80[14]	5.55[15]
$_{54}$Xe^{49+}	3.22[14]	8.78[15]	3.39[14]	1.32[16]	3.32[14]	5.91[15]	2.78[14]	6.56[15]	4.27[14]	7.87[15]	2.93[14]	1.34[16]	3.51[14]	1.19[16]	2.80[14]	9.46[15]

B. Relativistic radiative transition rates

The spontaneous probability for a discrete transition $i \to f$ in multipole expansion is given in perturbation theory by[5,10]

$$A_r(i \to f) = \frac{1}{2J_i+1} \sum_L \frac{2\pi}{2L+1} |\langle f||T_L||i\rangle|^2 . \qquad (5)$$

In the MCDF model,[6] the reduced multipole matrix element can be expressed in the CSF basis as follows:

$$\langle f||T_L||i\rangle = \sum_{\alpha=1}^{n_i} \sum_{\beta=1}^{n_f} C_{i\alpha}C_{f\beta}\langle \Phi(\Gamma_\beta J')||T_L||\Phi(\Gamma_\alpha J)\rangle .$$

$$(6)$$

This CSF matrix element in turn can be written as

$$\langle \Phi(\Gamma_\beta J')||T_L||\Phi(\Gamma_\alpha J)\rangle = \sum_{p,q} d_{pq}^L(\beta,\alpha)\langle p||T_L||q\rangle . \qquad (7)$$

Here, the one-electron reduced matrix elements $\langle p||T_L||q\rangle$ are as defined by Grant et al.[6] The $d_{pq}^L(\beta,\alpha)$ are angular factors.[11]

III. NUMERICAL CALCULATIONS

The wave functions and energies for bound states were evaluated using the MCDF model with the average-level (AL) scheme.[6] In AL calculations, the orbital wave functions are obtained by minimizing the average energy of all the levels with equal weight. In our present calculations for B-like ions, we used 35 CSF functions from $1s2s^22p^2$, $1s2s2p^3$, and $1s2p^4$ configurations for the initial autoionizing states. For the final Auger states, we used 10 CSF's from $1s^22s^2$, $1s^22s2p$, and $1s^22p^2$ configurations. For the final states of K x-ray transitions, 15 CSF's from $1s^22s^22p$, $1s^22s2p^2$, and $1s^22p^3$ configurations were included in the calculations. The mixing coefficients C_i [Eq. (3)] were obtained by diagonalizing the energy matrix which included Coulomb and transverse Breit interactions.[12] Quantum-electrodynamic corrections[12] were also included in the transition-energy calculations.

The transition energies were determined by performing separate MCDF calculations for initial and final ionic states and taking the energy difference. In the calculations of radial matrix elements, however, the orbital wave functions from the initial state were employed. The continuum wave functions for Auger calculations were generated by solving the Dirac-Fock equations corresponding to the final state without the exchange interaction between bound and continuum electrons. The angular factors of the Auger and radiative matrix elements were evaluated by using slightly modified general angular momentum subroutines.[6]

In order to study the effects of relativity, nonrelativistic transition rates in LS coupling were also computed by the multiconfiguration Hartree-Fock method, to be compared with the MCDF results. These nonrelativistic rates were calculated by repeating the MCDF procedure with the velocity of light increased one-thousandfold. The Auger and radiative rates were also calculated from single-configuration Dirac-Fock wave functions, in order to in-
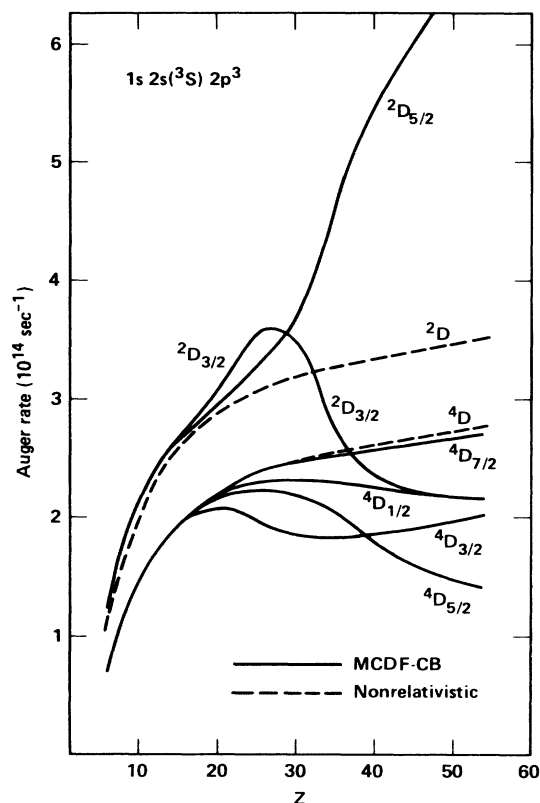
FIG. 1. Total Auger transition rates for ^2D and ^4D states of the $1s2s(^3S)2p^3$ configuration, as functions of atomic number. Solid curves represent results from MCDF calculations with Coulomb and Breit operator. Dashed curves indicate values from nonrelativistic calculations in LS coupling.

vestigate the effect of configuration interaction on these transition probabilities.

IV. RESULTS AND DISCUSSION

Total theoretical Auger and radiative transition rates, calculated in the length gauge, are listed in Tables I—III for states of the $1s2s^22p^2$, $1s2s2p^3$, and $1s2p^4$ configurations, respectively. The detailed transition energies and branching ratios will be published elsewhere.[13] In Figs. 1 and 2, the total Auger rates from the MCDF model including the contributions from the Coulomb and Breit operators in the Auger matrix elements are compared with results from nonrelativistic calculations. For $Z \geq 20$, the effect of relativity becomes quite pronounced; it can affect the Auger rates by as much as a factor of 2 for $Z \geq 40$. The Breit interaction can play a major role in the Auger decay of the high-spin states which are Auger forbidden in nonrelativistic LS coupling (cf. Figs. 3 and 4). The Breit interaction can become the sole contributor to opening an Auger channel, as for $1s2s^22p^2\,^4P_{5/2}$ $\rightarrow 1s^22s2p\,^3P_0$. Configuration interaction among states from the $1s2s^22p^2$ and $1s2p^4$ configurations is quite important for low-Z ions. This interaction can change individual Auger rates by as much as 70% (Fig. 5).
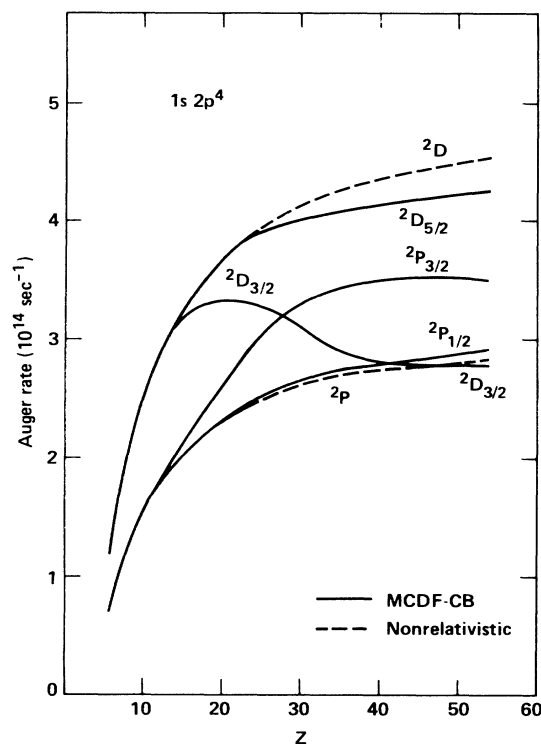

FIG. 2. Total Auger rates for ^2P and ^2D states of the $1s2p^4$ configuration, as functions of atomic number. See caption of Fig. 1 for details.
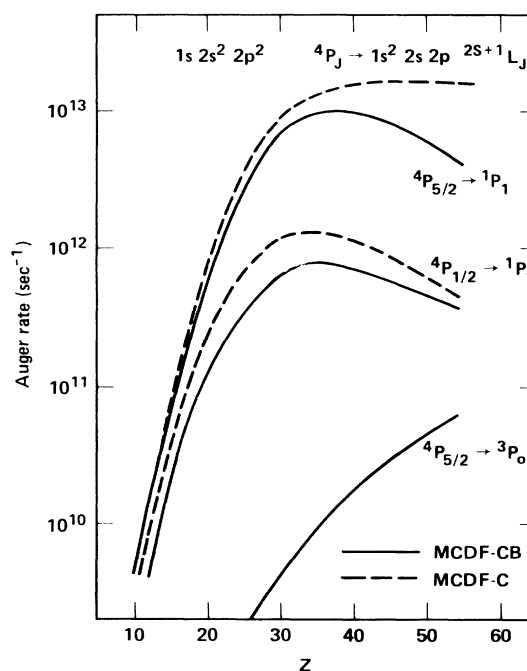

FIG. 3. Partial Auger rates for transitions from $1s2s^22p^2\,^4P_J$ to $1s^22s2p$ states, as functions of atomic number. Solid curves represent results from MCDF calculations including Coulomb and Breit interactions in the Auger matrix elements. Dashed curves indicate MCDF results in which only the Coulomb interaction is included.
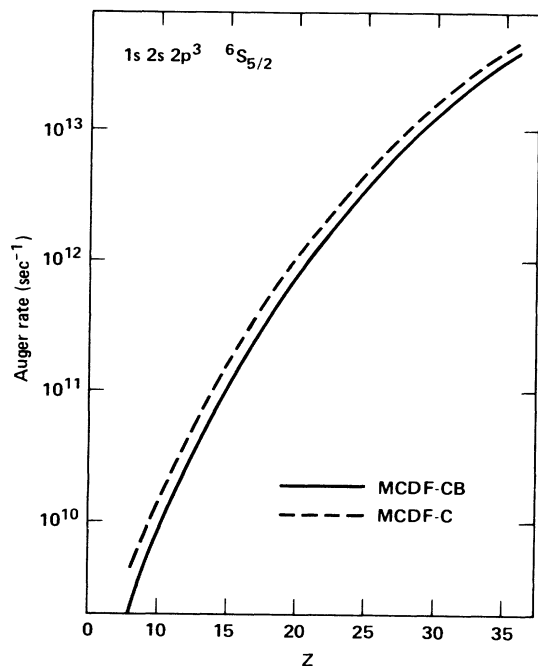
FIG. 4. Total Auger rate for the $1s2s2p^3\,{}^6S_{5/2}$ state, as a function of atomic number. See caption of Fig. 3 for details.
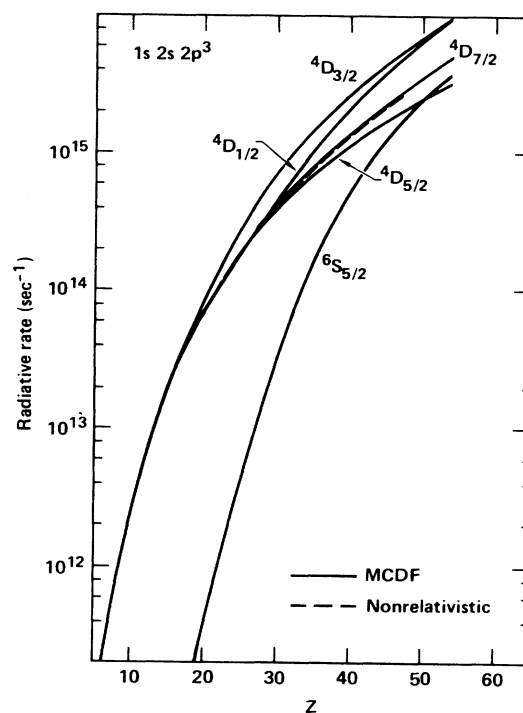

FIG. 6. Total radiative rates for ^4D and ^6S states of the $1s2s2p^3$ configuration, as functions of atomic number. Solid curves represent results from MCDF calculations. Dashed curves indicate predictions from nonrelativistic calculations in LS coupling.
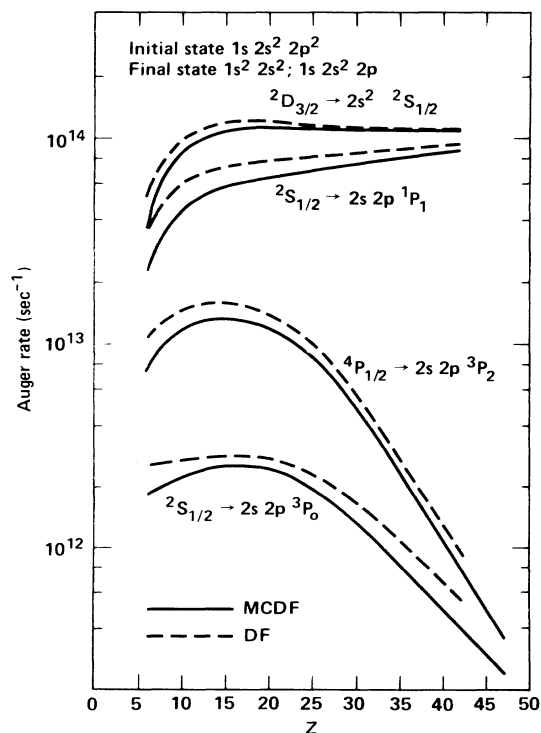

FIG. 5. Partial Auger rates for some states of the $1s2s^2 2p^2$ configuration, as functions of atomic number. Solid curves indicate results from MCDF calculations. Dashed curves represent values from single-configuration Dirac-Fock calculations.
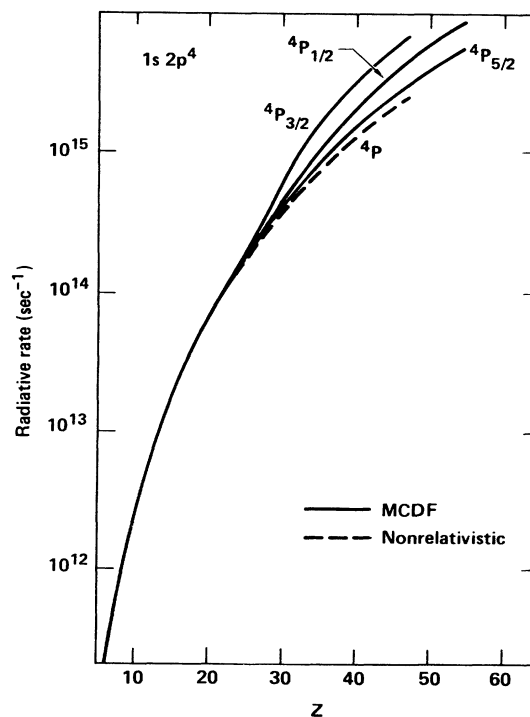

FIG. 7. Total radiative rates for the ^4P states of the $1s2p^4$ configuration, as functions of atomic number. See caption of Fig. 6 for details.
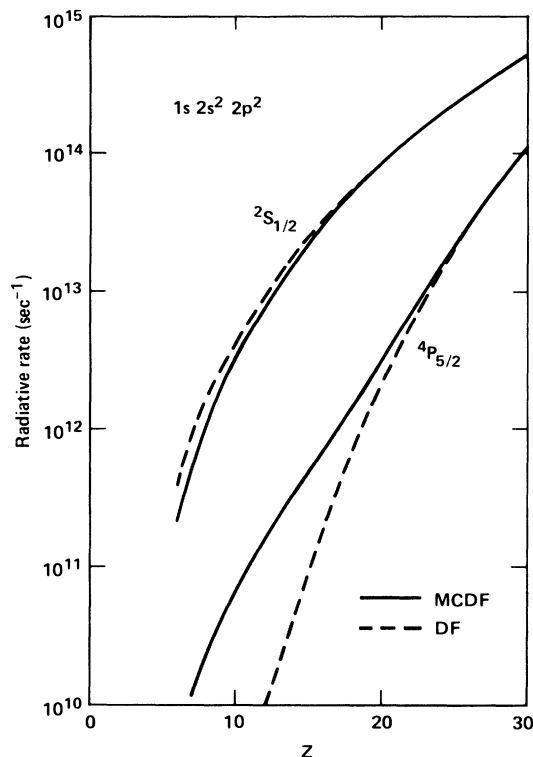
FIG. 8. Total radiative rates for $^3S_{1/2}$ and $^4P_{5/2}$ states of the $1s2s^22p^2$ configuration, as functions of atomic number. The solid curves indicates predictions from MCDF calculations; the dashed curves represent results from single-configuration Dirac-Fock calculations.

The effect of relativity on the radiative rates is displayed in Figs. 6 and 7. As for radiationless transitions, relativity begins to influence the rates for $Z \geq 20$; it can change the radiative rates by as much as a factor of 2 for $Z \geq 40$. For the $^6S_{5/2}$ state of the $1s2s2p^3$ configuration, the $E1$ transition is forbidden in the nonrelativistic LS-coupling limit. The transition becomes possible because of spin-orbit mixing with doublet and quartet states.

In Fig. 8, we compare the results from multiconfiguration Dirac-Fock and single-configuration Dirac-Fock calculations. For low-Z ions, the effect of configuration interaction reduces the radiative decay rate of the $1s2s^22p^2\,^2S_{1/2}$ state by as much as a factor of 2, and increases the radiative decay rate of the $1s2s^22p^2\,^4P_{5/2}$ state by an order of magnitude.

For the $1s2s^22p^2\,^4P_J$ states, electric-dipole ($E1$) photon emission is forbidden in LS coupling. This channel gains strength, however, from configuration mixing with the $1s2p^4\,^4P_J$ states, leading to $E1$ decay to the $1s^22p^3\,^4S_{3/2}$ state. The configuration-interaction effect becomes much less important for $Z \geq 20$.

We conclude that, for the states of the $1s2l^n2l'^m$ ($n + m = 4$) configurations of B-like ions, the configuration-interaction effect is quite important for low-Z ions, and the effect of relativity becomes very significant for atomic numbers above $Z \simeq 20$. These effects must be properly included in calculations of transition rates and of dielectronic satellite spectra. For low-Z ions, it may be necessary to include the effect of configuration interaction beyond the $n = 2$ complex, as well as the final continuum-channel interaction.[14]

ACKNOWLEDGMENTS

[1]L. A. Vainshtein and U. I. Safronova, At. Data Nucl. Data Tables 21, 49 (1978); 25, 311 (1980).

[2]U. I. Safronova and T. G. Lisina, At. Data Nucl. Data Tables 24, 49 (1979).

[3]M. H. Chen, B. Crasemann, and H. Mark, Phys. Rev. A 26, 1441 (1982); 27, 544 (1983).

[4]M. H. Chen, At. Data Nucl. Data Tables 34, 301 (1986).

[5]M. H. Chen, Phys. Rev. A 31, 1449 (1985).

[6]I. P. Grant, B. J. McKenzie, P. H. Norrington, D. F. Mayers, and N. C. Pyper, Comput. Phys. Commun. 21, 207 (1980).

[7]W. Bambynek, B. Crasemann, R. W. Fink, H.-U. Freund, H. Mark, C. D. Swift, R. E. Price, and P. Venugopala Rao, Rev. Mod. Phys. 44, 716 (1972).

[8]M. H. Chen, E. Laiman, B. Crasemann, and H. Mark, Phys. Rev. A 19, 2253 (1979).

[9]J. B. Mann and W. R. Johnson, Phys. Rev. A 4, 41 (1971).

[10]I. P. Grant, J. Phys. B 7, 1458 (1974).

[11]J. Hata and I. P. Grant, Phys. B 14, 2111 (1981).

[12]B. J. McKenzie, I. P. Grant, and P. H. Norrington, Comput. Phys. Commun. 21, 233 (1980).

[13]M. H. Chen and B. Crasemann (unpublished).

[14]H. P. Kelly, Phys. Rev. A 11, 556 (1975).